RSC Advances

ROYAL SOCIETY OF CHEMISTRY

www.rsc.org/advances

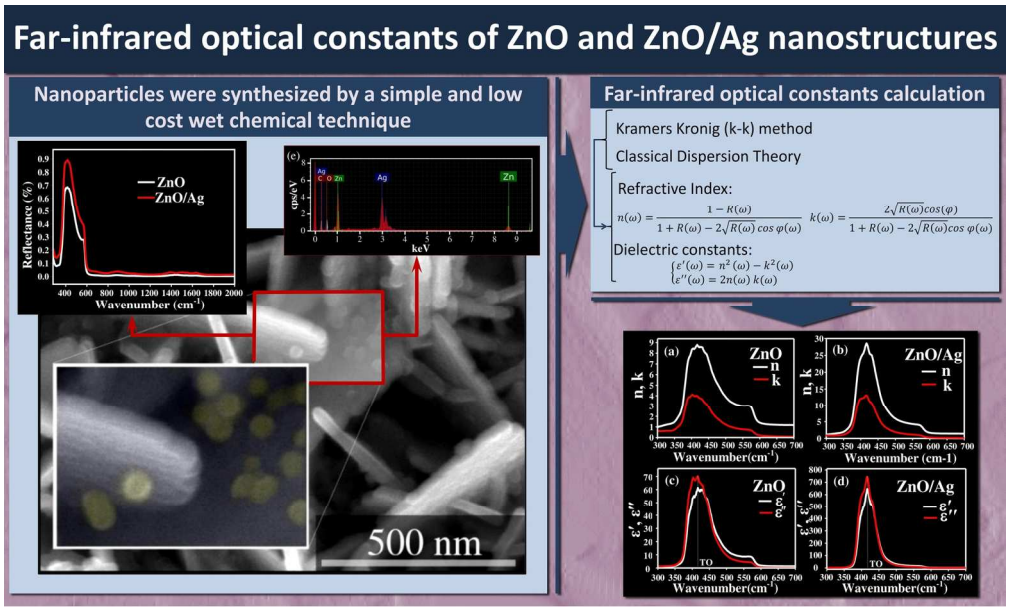

168x100mm (300 x 300 DPI)

Cite this: DOI: 10.1039/c0xx00000x

www.rsc.org/xxxxxx

ARTICLE TYPE

Far-Infrared Optical Constants of ZnO and ZnO/Ag nanostructures

Reza Zamiri,[a*] Avito Rebelo,[a] Golriz Zamiri,[b] Atena Adnani,[c] Ajay Kuashal,[a] Michael Scott Belsley,[d] J.M.F. Ferreira[a]

Received (in XXX, XXX) Xth XXXXXXXXX 20XX, Accepted Xth XXXXXXXXX 20XX

DOI: 10.1039/b000000x

We report on synthesis of ZnO nanoplates and ZnO nanoplates/Ag nanoparticles hetrostructures via simple and cost effective wet chemical precipitation method. The prepared samples were characterized for structural and optical properties by X-ray diffraction (XRD), Scanning Electron Microscopy (SEM), UV-VIS reflectance, Raman, and FT-IR spectroscopy. The Kramers–Kronig (K–K) method and classical dispersion theory was applied to calculate the Far-infrared optical constants such as, refractive index $n(\omega)$, dielectric constant $\varepsilon(\omega)$, transverse optical phonon (TO) and longitudinal (LO) optical phonon modes. We determined various optical constants values $n(\omega)$ and $\varepsilon(\omega)$for ZnO nanostructures in the range of 0 to 9 and 0 to 70, respectively. Whereas, on Ag deposition on ZnO nanostructures, the corresponding $n(\omega)$ and $\varepsilon(\omega)$values were found to be increase in the range of 0 to 30 and 0 to 800, respectively. The TO and LO optical phonon modes of ZnO nanoplates/Ag nanoparticles hetrostructure was also found to be higher (416 cm^{-1}, 620 cm^{-1}) when compared with corresponding values obtained for ZnO nanoplates (415 cm^{-1}, 604 cm^{-1}).

A Introduction

Recently, semiconductor/metal composites materials have been attracted wide scientific and technological interest due to their unique electrical, optical and catalytic properties, which in turn make them suitable candidate for potential applications in optoelectronic devices [1-5]. ZnO is a wide band gap (3.37 eV at room temperature) semiconductor, and has been studied by numerous researchers during the past 20 years [6-10]. Metals such as Ag and Au have electron storage properties which consecutively make possible to develop charge separation in semiconductor/metal composite systems [3-5]. The suitability of ZnO/Ag based composites for photovoltaic devices has stimulated great interest in the preparation and characterization of this material. In ZnO/Ag heterostructures, Ag displays sharp surface plasmon resonance peak in the visible region of electromagnetic spectra with a favorable frequency dependence of the real and imaginary parts of the dielectric function [11-14]. By reducing size of composite material to nano-scale can change optical properties of materials such as optical dispersion, transmission and reflection via scattering and interference [15,16]. Searching new routes for synthesis and processing of nano-scale hetrostructures and understanding the relationship between the structures and the properties are part of an emerging and rapidly growing field of nanotechnology [17-21]. There are reports on synthesis of ZnO/Ag hetrostructures with different morphologies such as Ag/ZnO nanofibers, Ag/tetrapod-like ZnO whisker nanocompounds, Ag nanoparticles-stabilized ZnO nanosheets and Ag nanoparticles/ZnO nanorods [22-24]. Core/shell Ag/ZnO and ZnO/Ag nanostructures have also been derived from various routes [25, 27]. In addition, deposition of Ag nanoparticles onto pre-synthesized ZnO nanorods leads to an enhancement of Raman signals and photocatalytic activity [28, 29]. The evaluation of optical constants of ZnO based hetrostructures is of considerable importance for applications in integrated optic devices such as switches, filters and optical testers, etc., where the refractive index of a material is the key parameter for device design. The limited degree of precision in optical devices is due to variation in optical properties of a material, including, most specifically, the real and the imaginary parts of the effective complex index of refraction, commonly known as effective optical constants $n(\omega)$ and $k(\omega)$ [30]. Precise information on optical properties of ZnO/Ag nanocomposite such as dielectric response to electromagnetic waves in infrared region is essential importance and much desired.

Earlier we have reported on synthesis of ZnO/Ag core/shell nanocomposite by laser ablation technique in liquid media, in which ZnO nanoparticles act as the core and Ag acts as the shell [10]. In the present study, ZnO nanoplates /Ag nanoparticles hetrostructure have been grown via a simple and cost effective chemical route. Novelty of our chemical route approach is synthesis of complex ZnO/Ag nanostructures without any need of growth template. It is demonstrated that this chemical route is a viable option to obtain ZnO/Ag nano scale hetrostructures with good optical properties which will further benefits material research and optoelectronic device applications. The optical properties of the synthesized ZnO/Ag nanocomposites has been systematically investigated in Far infrared region as infrared

spectroscopy is provide insight into dynamical process related to phonons, charge carriers, spin and their coupling process.

B Experimental

ZnO nanoplates were prepared by a wet chemical precipitation method. Firstly, 3.352 g of $ZnCl_2$ (Aldrich, Germany) was dissolved in distilled water. The obtained solution was dropped into 100 mL of 0.1 M NaOH (Merk, Germany) solution. For the synthesis of the ZnO/Ag nanostructures, 0.01 M Ag (NO_3) (Aldrich, Germany) was added in vessel containing precipitated ZnO nanostructures. The obtained solution was further stirred for 2 h. Thereafter, $NaBH_4$ solution of 0.1M was added in stirred solution as a reducing agent to convert Ag ions into Ag particles. The resulting mixture was further kept under continuous stirring for 2 h. The pH value of the solutions was kept nearly in the range of 13-14. Finally in order to obtain the solid phase separation from the liquid phase, the precipitated materials in suspensions were ultra–centrifuged (10,000 rpm, 10 min) to obtain clear supernatant liquids. The obtained solid phases (both ZnO nanoplates and ZnO/Ag nanostructures) were then washed thoroughly in distilled water to remove the unwanted ions (Na^+, Cl^-, NO_3^-). Washing solid precipitates was repeated several times up to getting a Na^+ concentration below to 0.66 ppm measured by atomic absorption spectroscopy, followed by drying at 80 ºC for 24 h. The structure and morphology of the samples were studied by X-ray diffraction (Shimadzu XRD-6000, Tokyo, Japan) and Scanning Electron Microscopy (SEM, SU-70, Hitachi), respectively. The optical properties of the samples were measured by using UV–visible (Perkin-Elmer, Lambda 35), Raman and FT-IR spectrometry.

C Results and discussions

Figure 1 shows the XRD patterns of ZnO and ZnO/Ag nanostructures. The XRD pattern of ZnO shows the presence of a well crystalline hexagonal wurtzite phase (JCPDS, no. 36-1451), whereas, ZnO/Ag nanostructure exhibits the ZnO wurtzite phase and three additional peaks at 38.1°, 44.2° and 64.4° related to (1 1 1), (2 0 0) and (2 2 0) planes of Ag nanoparticles corresponding

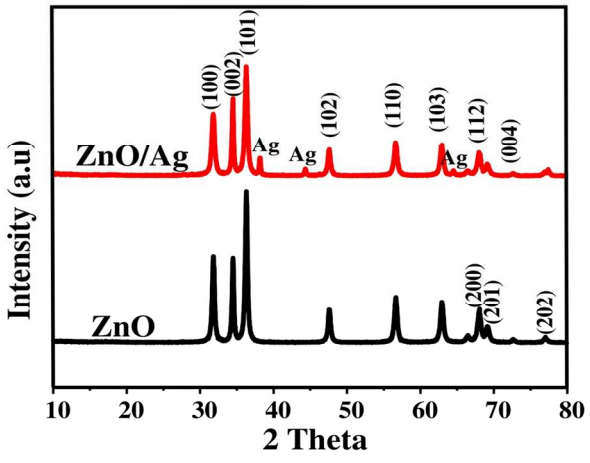

Fig. 1 XRD patterns of ZnO and ZnO/Ag nanostructures.

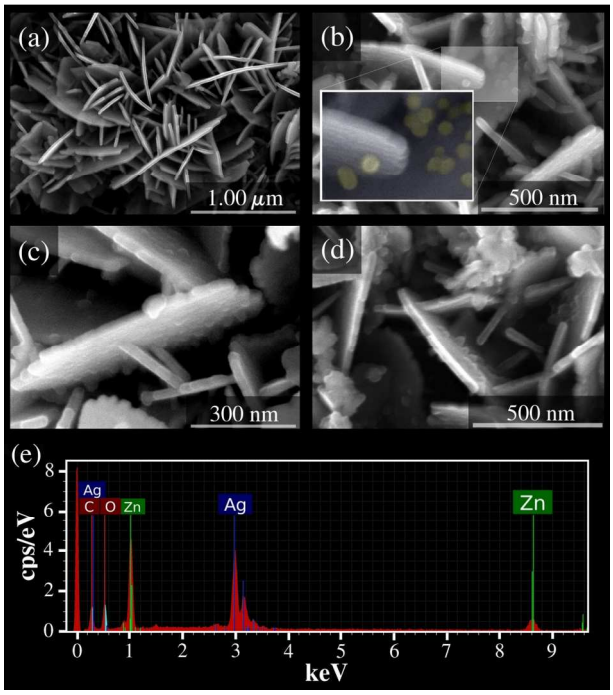

Fig. 2 SEM images of (a) ZnO, (b-d) ZnO/Ag nanostructures and (e) EDS analysis of ZnO/Ag nanostructures.

to face-centered cubic (fcc) metallic Ag phase (JCPDS no. 04-0783). Appearance of Ag peaks in the XRD diffraction pattern clearly confirmed the formation of crystalline silver nanoparticles.

The morphologies of the prepared nanostructures were further studied from SEM analysis. Figure 2 shows SEM images of ZnO nanostructures (Fig. 2a), and ZnO/Ag nanostructures (Fig. 2(b-d)). Nano-sized plate like structures has been obtained for both ZnO and ZnO/Ag composites. However, distribution of Ag particles all over the surfaces of ZnO nanoplates has been observed in ZnO/Ag nanocomposites samples (as shown in Fig. 2b-2d). The presence of Ag content was further confirmed by EDS analysis of ZnO/Ag nanostructures. The obtained EDS spectra are shown in Fig. 2e which shows the presence of Ag, Zn and O in the final products. The absence of extra impurity peaks in EDS spectra suggests the purity of obtained nanostructures with no sign of any additives left in final obtained solid precipitates.

Figure 3 shows the reflectance spectra of prepared ZnO and ZnO/Ag nanostructures in UV-VIS range of electromagnetic wavelengths. An abrupt change in reflectance behaviour at a wavelength around 385 nm was observed in both the samples, which is assigned to recombination of electron holes in ZnO. In addition, the specific surface plasmon resonance absorption peak of Ag nanoparticles was also observed at around 513 nm as shown in ZnO/Ag nanostructures reflectance behavior.

The surface plasmon peak location of a metal can be calculated by the following equation [31].

$$\lambda_p = [4\pi^2 c^2 m_{eff} \varepsilon_0 / N e^2]^{1/2} \quad (1)$$

Where, m_{eff} and N are the effective mass and electron density respectively. Red shift in surface plasmon resonance peak has been observed as usually it is at ~400 nm for Ag [32, 33]. The

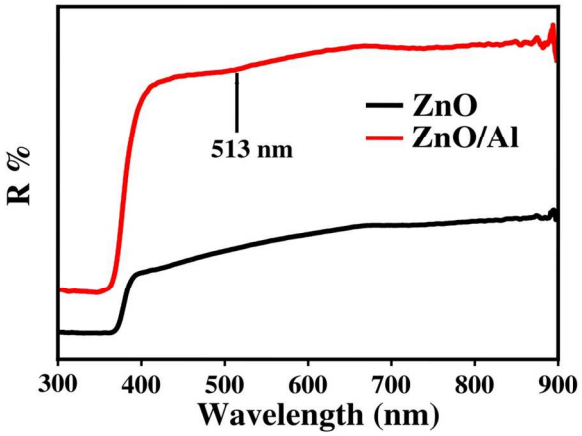

Fig. 3 Reflectance spectra of ZnO and ZnO/Ag nanostructures in visible range of electromagnetic wavelengths.

observed red shift in surface plasmon resonance peak indicating reduction in electron density of Ag in ZnO/Ag nanostructures. This reduction can be explained according to the Fermi energy levels of ZnO and Ag, as the ZnO work function (4.3 eV) is larger than Ag (4.1 eV), therefore the Fermi level of ZnO is located lower to Ag Fermi level. This leads to easy electrons transfer from Ag nanoparticles to ZnO nanoplates, when the two systems are not in equilibrium.

Figure 4 indicates the Raman spectra of prepared ZnO and ZnO/Ag nanostructures excited by λ = 1064 nm laser source. Two strong peaks were found for ZnO and ZnO/Ag nanostrucutres located at 430 cm^{-1} and 580 cm^{-1} corresponding to E2 and *E*1(LO) modes of wurtzite ZnO structure respectively [34]. The 437 cm^{-1} peak disappears in ZnO/Ag nanostructure due to overlapping with other stronger resonant Raman scattering peaks. It can be clearly seen that the peaks intensity of ZnO/Ag nanostructure is higher than that observed for ZnO nanostructure. There are two theories which can be applied to explain the enhancement of the peak intensity on Ag deposition on ZnO nanoplates as: 1) the electromagnetic theory which is based on

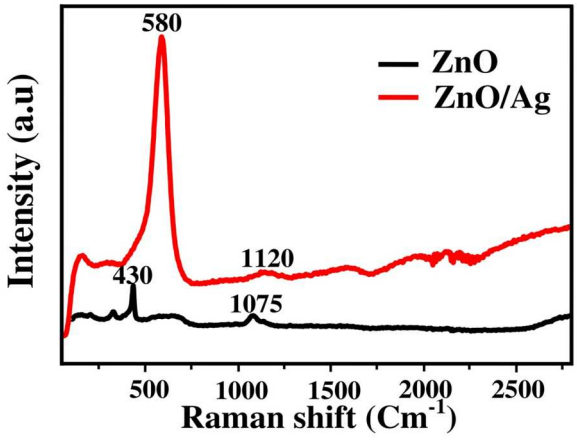

Fig. 4 Raman spectra of the ZnO and ZnO/Ag nanostructures.

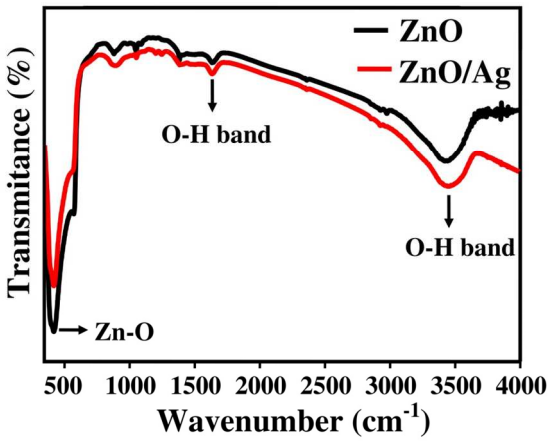

Fig. 5 FT-IR spectrum of ZnO and ZnO/Ag nanostructures.

the excitation of localized surface plasmons; 2) chemical theory which rationalizes the effect through the formation of charge transfer complexes and only applies for species which have formed a bond with the surface. The Raman intensity is relative to the intensity of the locally formed *E*-field which can interact with optical phonons and enhances the scattering intensity of active phonons [31]. Therefore, the enhancement of Raman intensity for ZnO/Ag nanostructures is due to strong local *E*-field at the interface between ZnO and Ag. The intensity of interaction among ZnO and Ag is determined by the polarization induced in each one due to the *E*-field arising from the charge separation, as the positive ions left on the Ag nanoparticles surface after electrons transfer to the ZnO.

Figure 5 shows FT-IR spectrum of ZnO and ZnO/Ag nanostructures. The strong absorption band ranging from 400 cm^{-1} to 500 cm^{-1} is assigned to Zn-O stretching vibration mode of the ZnO nanoplates and intensity of this peak is reduced after formation of Ag nanoparticles on the surface of ZnO nanoplates [35]. There are also broad peaks at 3450 cm^{-1} and 1630 cm^{-1}, corresponding to the hydroxyl groups due to the adsorption of water on the particles surface [36]. No vibration mode in relation with Ag was observed in the spectrum of ZnO/Ag nanostructure, which indicates that there is no chemical bonding between Ag and ZnO.

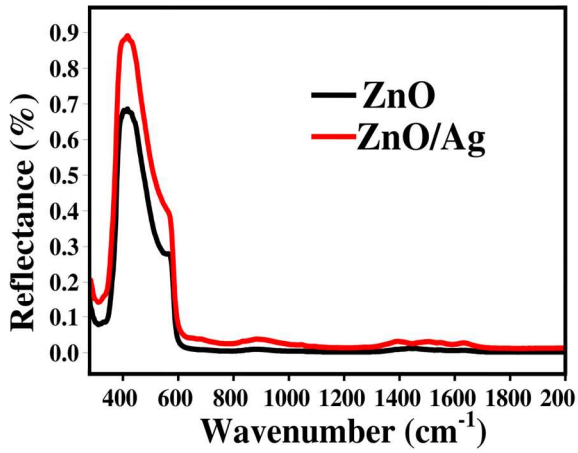

Fig. 6 Reflectance spectra of ZnO and ZnO/Ag nanostructures.

The K–K method was applied on FT-IR reflectance spectra data to evaluate the Far-inferred optical constants of the prepared ZnO and ZnO/Ag nanostructures. . The experimentally measured reflectance spectra of ZnO and ZnO/Ag nanostructures are shown in Figure 6. The reflective index n is an important physical quantity in optical design and generally is a complex quantity:

$$\tilde{n}(\omega) = n(\omega) + ik(\omega) \qquad (2)$$

Where $n(\omega)$and $k(\omega)$ are the real and the imaginary parts of the complex refractive index respectively, and can be obtained by the following equations [37]:

$$n(\omega) = (1 - R(\omega))/(1 + R(\omega) - 2\sqrt{(R(\omega))}\ \cos\varphi(\omega)) \quad (3)$$

$$k(\omega) = (2\sqrt{(R(\omega))}\cos(\varphi))/(1 + R(\omega) - 2\sqrt{(R(\omega))}\cos\varphi(\omega)) \quad (4)$$

Here, $\varphi(\omega)$ is the phase change between the incident and the reflected signal at a particular wave number, ω and $R(\omega)$ is the reflectance in that wave number, ω. The phase change can be calculated from the K–K dispersion relation given by [38]:

$$\varphi(\omega) = (-\omega)/\pi \int_0^{\infty} (LnR(\omega') - LnR(\omega))/(\omega'^2 - \omega^2)\, d\omega' \qquad (5)$$

This integral can further be precisely evaluated by using Maclaurin's method as [39]:

$$\varphi(\omega_j) = (4\omega_j/\pi) \times \Delta\omega \times \sum_i (\ln\left(\sqrt{R(\omega)}\right))/(\omega_i^2 - \omega_j^2) \qquad (6)$$

here $\Delta\omega = \omega_{j+1} - \omega_j$ and if j is an even number then i=1, 3, 5, 6, ,...$j-1$, $j+1, \ldots..$ while, if j is an odd number then i =2, 4, 6,...$j-1$, $j+1, \ldots..$

In addition, the dielectric function can be obtained by the square of the refractive index. Therefore, the real and imaginary parts of the complex dielectric function are given by:

$$\varepsilon = [\tilde{n}(\omega)]^2 = [n(\omega) + ik(\omega)]^2$$
$$\Rightarrow \varepsilon' + i\varepsilon'' = n^2(\omega) - k^2(\omega) + 2in(\omega)k(\omega)$$
$$\Rightarrow \{\varepsilon'(\omega) = n^2(\omega) - k^2(\omega);\ \varepsilon''(\omega) = 2n(\omega)k(\omega) \qquad (7)$$

The calculated optical constant values of ZnO and ZnO/Ag nanostructures obtained using equations 2 to 7 are shown in Fig. 7(a&b). The strong peaks were observed for $n(\omega)$ and $k(\omega)$ at around 415 cm^{-1} and 410 cm^{-1}, respectively. However, the intensity of the peaks for both $n(\omega)$and $k(\omega)$ increased from n_{max} = 8.80, and k_{max} = 4.16 (for ZnO nanostructures) to n_{max} = 28.80, k_{max} = 13.30 (for ZnO/Ag nanostructures). This increase in intensity values could be due to the formation of Ag nanoparticles on the surface of ZnO nanoplates which causes the reduction of the Zn-O absorption band intensity in the far infrared region. The calculated values of real and imaginary parts of the dielectric function of the prepared samples are also shown in Fig. 7c and 7d. It can be seen that the value of maximum dielectric function was drastically increased for ZnO/Ag nanostructures compared to ZnO nanostructures. Therefore, it can be concluded that the presence of Ag nanoparticles on the surface of ZnO nanoplate can improve optical properties of ZnO in Far infrared region.

Till date, there are certain reports on optical properties of bulk

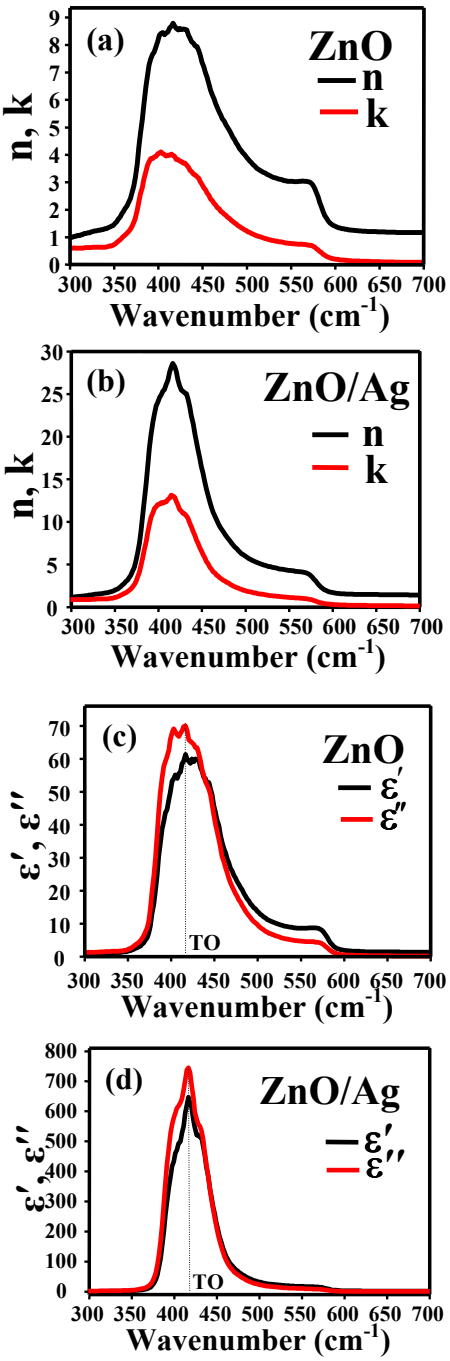

Fig. 7 (a, b) refractive index and extinction coefficient, (c, d) real and imaginary parts of dielectric functions of ZnO and ZnO/Ag nanostructures.

and nanostructured ZnO in infrared region and the field is still wide open as per its potential in device application [40-47]. For example, Garc´ıa-Serrano et al. [41] used Far infrared (FIR) reflectance spectra for the qualitative determination of free carrier density in metal and semiconductor nanoclusters embedded ZnO films. On the other hand, Yamamoto et al.[42] focused on the optical surface phonon modes in small ZnO crystals using FIR transmission measurements at room temperature. In addition, terahertz time-domain spectroscopy was used to determine

Table 1 Various TO and LO optical phonons values of ZnO and ZnO/Ag nanostructures

samples	Transfer optical phonon (TO),cm^{-1}	Longitude optical phonon (LO), cm^{-1}
ZnO	415	604
ZnO/Ag	416	620

refractive index, dielectric constant and absorption coefficient of bulk and nanostructured ZnO in the FIR region and it was found that ZnO nanostructures exhibit very similar phonon resonances with that of single-crystal ZnO [44, 45]. Polarized FIR reflectance technique has also been applied by researchers to study the optical properties of pure and Mn doped ZnO nanoparticles prepared by sol gel method [47]. They report optical constant values i.e. refractive index (n) and dielectric constants (ε) values in the range between 1 to 7 and -25 to 35, respectively. We determined various optical constants values n and ε for ZnO nanostructures in the range of 0 to 9 and 0 to 70, respectively. However, on Ag deposition on ZnO nanostructures, the corresponding n and ε values were found to be increase in the range of 0 to 30 and 0 to 800, respectively.

The TO and LO modes of a material are useful to illustrate the optical interactions with the lattice. TO mode frequencies corresponds to the frequency at which imaginary part of the dielectric function shows a peaks (Fig.7c and 7d) [48]. The LO mode frequencies can be obtained by plotting the imaginary part of $-1/\varepsilon$ behaviour against wavenumber as shown in Fig. 8a and 8b. Frequency at which peak observed in figure 8, corresponds to LO mode frequency. Table 1 illustrates various TO and LO optical phonons values obtained for prepared ZnO and ZnO/Ag nanostructures.

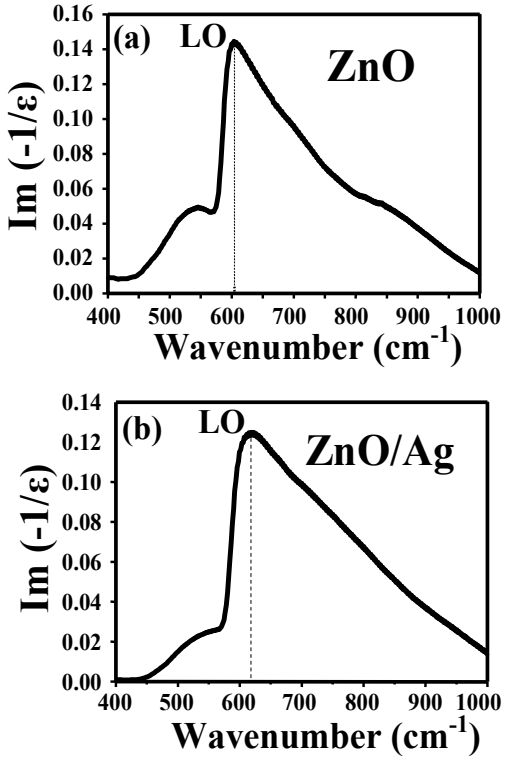

Fig. 8 Imaginary part of $-1/\varepsilon$ behaviour with wavenumber for ZnO and ZnO/Ag nanostructures.

Conclusions

ZnO nanoplates and ZnO nanoplates/Ag nanoparticles hetrostructures have been successfully synthesized via cost effective wet precipitation method. The presence of Ag in ZnO/Ag nanocomposites was confirmed by the presence of extra phases along with wurtzite ZnO phase in XRD spectra and by taking EDS spectra. Nano-sized plates like structure were observed in SEM images of the prepared samples. An absorption peak observed in reflectance spectra of ZnO/Ag sample at a wavelength of ~ 513 nm corresponds to surface Plasmon resonance of Ag nanoparticles. Raman peak intensity was found to be higher in case of ZnO/Ag nanostructures when compared with Raman intensity observed for ZnO nanostructures. The Far-infrared optical constants of the prepared samples were successfully calculated by using Kramers–Kronig method. Far infrared optical properties of ZnO nanoplates were found to enhance when Ag is deposited on surface of ZnO nanoplates making it as ZnO/Ag nanocomposites. The enhancement in optical properties of ZnO will further benefit its potential use in various optical devices.

Acknowledgments

Authors, Reza Zamiri and A. Kaushal would like to thank the Foundation for Science and Technology of Portugal (FCT) for the financial support under the grant references, SFRH/BPD/76185/2011 and SFRH/BPD/77598/2011, respectively. The authors would also like to thank CICECO for the work at the University of Aveiro.

Notes and **References**

[a]*Department of Materials Engineering and Ceramic, University of Aveiro, Campus Santiago, 3810-193 Aveiro, Portugal*
E-mail: zamiri.r@gmail.com
[b]*School of Civil Engineering, K.N. Toosi, University of Technology, Tehran, Iran*
[c]*Department of Analytical Chemistry, Faculty of Chemistry,University of Mazandaran, Babolsar, Iran.*
[d]*CFUM, Department of Physics, University of Minho, 4710-059, Braga, Portugal.*

1. Merga, G., et al., Probing silver nanoparticles during catalytic H2 evolution.Journal of the American Chemical Society, 2008.**130**(22): p. 7067-7076.
2. Choi, J.-s., et al., Biocompatible heterostructured nanoparticles for multimodal biological detection.Journal of the American Chemical Society, 2006.**128**(50): p. 15982-15983.
3. Sun, K., et al., Solution synthesis of large-scale, high-sensitivity ZnO/Si hierarchical nanoheterostructure photodetectors. Journal of the American Chemical Society, 2010.**132**(44): p. 15465-15467.

4. Li, X. and Y. Wang, Structure and photoluminescence properties of Ag-coated ZnO nano-needles.Journal of Alloys and Compounds, 2011.**509**(19): p. 5765-5768.
5. Sahu, R.K., et al., Stabilization of intrinsic defects at high temperatures in ZnO nanoparticles by Ag modification.Journal of colloid and interface science, 2012.**366**(1): p. 8-15.
6. Zamiri, R., et al., Er doped ZnO nanoplates: Synthesis, optical and dielectric properties.Ceramics International, 2014.**40**(1): p. 1635-1639.
7. Zamiri, R., et al., Effects of rare-earth (Er, La and Yb) doping on morphology and structure properties of ZnO nanostructures prepared by wet chemical method.Ceramics International, 2013.
8. Zamiri, R., et al., Electrical properties of Ag-doped ZnOnano-plates synthesized via wet chemical precipitation method.Ceramics International, 2014.**40**(3): p. 4471-4477.
9. Zamiri, R., et al., Aqueous starch as a stabilizer in zinc oxide nanoparticle synthesis via laser ablation. Journal of Alloys and Compounds, 2012.**516**: p. 41-48.
10. Zamiri, R., et al., Laser assisted fabrication of ZnO/Ag and ZnO/Au core/shell nanocomposites. Applied Physics A, 2013: p. 1-7.
11. Yin, Y., W. Que, and C. Kam, ZnO nanorods on ZnO seed layer derived by sol–gel process.Journal of sol-gel science and technology, 2010.**53**(3): p. 605-612.
12. Sun, Y., et al., Synthesis of aligned arrays of ultrathin ZnO nanotubes on a Si wafer coated with a thin ZnO film.Advanced materials, 2005.**17**(20): p. 2477-2481.
13. Jiang, C., et al., Improved dye-sensitized solar cells with a ZnO-nanoflower photo anode. Applied Physics Letters, 2007.**90**(26): p. 263501-263501-3.
14. Elias, J., et al., Conversion of ZnO nanowires into nanotubes with tailored dimensions.Chemistry of materials, 2008.**20**(21): p. 6633-6637.
15. Du, W., et al., Ultrathin β-In2S3 nanobelts: shape-controlled synthesis and optical and photocatalytic properties.Crystal Growth and Design, 2008.**8**(7): p. 2130-2136.
16. Panda, A.B., et al., Synthesis, assembly, and optical properties of shape-and phase-controlled ZnSe nanostructures.Langmuir, 2007.**23**(2): p. 765-770.
17. Kim, H.W., K.M. Kang, and H.-Y. Kwak, Preparation of supported Ni catalysts with a core/shell structure and their catalytic tests of partial oxidation of methane.International Journal of Hydrogen Energy, 2009.**34**(8): p. 3351-3359.
18. Yang, P., et al., Fabrication and luminescent properties of the core–shell structured YNbO< sub> 4</sub>: Eu< sup> 3+</sup>/Tb< sup> 3+</sup>@ SiO< sub> 2</sub> spherical particles.Journal of Solid State Chemistry, 2008.**181**(8): p. 1943-1949.
19. Ma, Z., et al., Synthesis and characterization of multifunctional silica core–shell nanocomposites with magnetic and fluorescent functionalities.Journal of magnetism and magnetic materials, 2009.**321**(10): p. 1368-1371.
20. Lu, Y., C.-L. Yan, and S.-Y. Gao, Preparation and recognition of surface molecularly imprinted core–shell microbeads for protein in aqueous solutions.Applied Surface Science, 2009.**255**(12): p. 6061-6066.
21. Liu, H., et al., Electrochemical performance of LiFePO< sub> 4</sub> cathode material coated with ZrO< sub> 2</sub>nanolayer.Electrochemistry communications, 2008.**10**(1): p. 165-169.
22. Zhang, D., X. Liu, and X. Wang, Growth and photocatalytic activity of ZnOnanosheets stabilized by Ag nanoparticles.Journal of Alloys and Compounds, 2011.**509**(15): p. 4972-4977.
23. Hu, H., et al., ZnO/Ag heterogeneous structure nanoarrays: Photocatalytic synthesis and used as substrate for surface-enhanced Raman scattering detection.Journal of Alloys and Compounds, 2011.**509**(5): p. 2016-2020.
24. Yin, X., W. Que, and F. Shen, ZnO nanorods arrays with Ag nanoparticles on the (002) plane derived by liquid epitaxy growth and electrodeposition process.Thin Solid Films, 2011.**520**(1): p. 186-192.
25. Li, F., et al., Synthesis and characterization of ZnO–Ag core–shell nanocomposites with uniform thin silver layers.Applied Surface Science, 2010.**256**(20): p. 6076-6082.
26. Song, C., et al., Facile synthesis of Ag/ZnO microstructures with enhanced photocatalytic activity.Materials Letters, 2010.**64**(14): p. 1595-1597.
27. Zheng, Y., et al., Ag/ZnOheterostructure nanocrystals: synthesis, characterization, and photocatalysis.Inorganic chemistry, 2007.**46**(17): p. 6980-6986.
28. Yin, X., et al., Ag nanoparticle/ZnO nanorods nanocomposites derived by a seed-mediated method and their photocatalytic properties.Journal of Alloys and Compounds, 2012.**524**: p. 13-21.
29. Chen, C., et al., Enhanced Raman scattering and photocatalytic activity of Ag/ZnOheterojunction nanocrystals.Dalton Transactions, 2011.**40**(37): p. 9566-9570.
30. Rakic, A., et al., Optical properties of metallic films for vertical-cavity optoelectronic devices. Applied Optics, 1998. **37**: p. 5271-5282.
31. Shan, G., et al., Enhanced Raman scattering of ZnO quantum dots on silver colloids.The Journal of Physical Chemistry C, 2007.**111**(8): p. 3290-3293.
32. Zamiri, R., et al., Fabrication of silver nanoparticles dispersed in palm oil using laser ablation.International journal of molecular sciences, 2010.**11**(11): p. 4764-4770.
33. Zamiri, R., et al., Laser-fabricated castor oil-capped silver nanoparticles.International journal of nanomedicine, 2011.**6**: p. 565.
34. Cheng, H.-M., et al., Raman scattering and efficient UV photoluminescence from well-aligned ZnO nanowires epitaxially grown on GaN buffer layer.The Journal of Physical Chemistry B, 2005.**109**(18): p. 8749-8754.
35. Das, J. and D. Khushalani, Nonhydrolytic route for synthesis of ZnO and its use as a recyclable photocatalyst.The Journal of Physical Chemistry C, 2010.**114**(6): p. 2544-2550.
36. Pillai, S.C., et al., Synthesis of high-temperature stable anatase TiO2 photocatalyst.The Journal of Physical Chemistry C, 2007.**111**(4): p. 1605-1611.
37. Harris, D.C. and M.D. Bertolucci, Symmetry and Spectroscopy: An Introduction to Vibrational and Electronic Spectrosocpy. 1978: DoverPublications. com.
38. Lu carini, V., et al., Kramers-Kronig Relations in Optical Materials Research. 2005. Springer Series in Optical Sciences.
39. Ghasemifard, M., S. Hosseini, and G.H. Khorrami, Synthesis and structure of PMN–PT ceramic nanopowder free from pyrochlore phase.Ceramics International, 2009.**35**(7): p. 2899-2905.
40. Kim J, Jung S, Choi EJ, Kim K, Lee K, Im S. Infrared spectroscopy of the interface charge in a ZnO field-effect transistor. Applied Physics Letters. 2008;93(24):241902.
41. García-Serrano J, Casarrubias-Segura G, Galindo AG, Mathew X, Pal U. Infrared study of free carriers in X/ZnO (X=semiconductor, metal) nanocomposites. Thin Solid Films. 2005;490(2):137-41.

42. Yamamoto K, Tran C-D, Shimizu H, Abe K. Optical Surface Phonon Modes in ZnO Small Crystals. Journal of the Physical Society of Japan. 1977;42(2):587-90.
43. Lavrov EV. Infrared absorption spectroscopy of hydrogen-related defects in ZnO.Physica B: Condensed Matter. 2003;340-342:195-200.
44. Azad AK, Han J, Zhang W. Terahertz dielectric properties of high-resistivity single-crystal ZnO. Applied Physics Letters. 2006;88(2):021103.
45. Han JG, Azad AK, Zhang WL. Far-infrared characteristics of bulk and nanostructured wide-bandgap semiconductors.Journal of Nanoelectronics and Optoelectronics. 2007;2(3):222-33.
46. PohkokOoi SLSNZHHAH. Far Infrared Optical Properties of Bulk Wurtzite Zinc Oxide Semiconductor.Journal of Materials Sciences and Technology. 2011;27(5):465-70.
47. Abrishami ME, Hosseini SM, Kakhki EA, Kompany A, Ghasemifard M. synthesis and structure of pure and mn-doped zinc oxide nanopowders. International Journal of Nanoscience. 2010;09(01n02):19-28.
48. Ng S, Hassan Z, Abu Hassan H. Kramers–Kronig analysis of infrared reflectance spectra with a single resonance. JurnalTeknologi. 2012;44(1):67–76.